Reversible Optical Control of Monolayers on Water through Photoswitchable Lipids

ARTICLE *in* THE JOURNAL OF PHYSICAL CHEMISTRY B · FEBRUARY 2011

Impact Factor: 3.3 · DOI: 10.1021/jp1113619 · Source: PubMed

5 AUTHORS, INCLUDING:

Bert Poolman
University of Groningen
267 PUBLICATIONS **10,975** CITATIONS
SEE PROFILE

Mischa Bonn
Max Planck Institute for Polymer Research
347 PUBLICATIONS **7,477** CITATIONS
SEE PROFILE

THE JOURNAL OF PHYSICAL CHEMISTRY B

ARTICLE

pubs.acs.org/JPCB

Reversible Optical Control of Monolayers on Water through Photoswitchable Lipids

Ellen H. G. Backus,[†] Johanna M. Kuiper,[‡] Jan B. F. N. Engberts,[‡] Bert Poolman,[‡] and Mischa Bonn*[,†]

[†]FOM Institute AMOLF, Science Park 104, 1098 XG Amsterdam, The Netherlands

[‡]Departments of Biochemistry and Synthetic-Organic Chemistry, Stratingh and Zernike Institute, University of Groningen, Nijenborgh 4, 9747 AG Groningen, The Netherlands

ABSTRACT: We have obtained molecular insights into a monolayer of azobenzene-based photoswitchable lipids self-assembled on water, using the surface sensitive technique vibrational sum-frequency generation spectroscopy in combination with surface pressure measurements. The photolipids can undergo wavelength-dependent, light-triggered cis/trans and trans/cis isomerization, allowing for reversible control of the surface pressure and the molecular ordering of the lipids in the monolayer. If the photoswitchable lipid is embedded in a layer with conventional phospholipids, such as 1,2-dipalmitoyl-*sn*-glycero-3-phosphocholine (DPPC), we show that the surface pressure and molecular ordering of DPPC can be influenced by switching the azobenzene-based lipid between its two states. Remarkably, the state with the higher surface pressure (cis-state) is characterized by a lower degree of molecular order. This counterintuitive result can be understood by noting that the azobenzene moiety in the cis state has a higher dipole moment and therefore favors interaction with water. The surface free energy of the system is lowered (increase of surface pressure) by electrostatic interactions with the lipid headgroups at the interface, resulting in a loop formation of the lipid tail with the *cis*-azobenzene. This disorder in the tail of the photoswitchable lipid perturbs as well the ordering of DPPC.

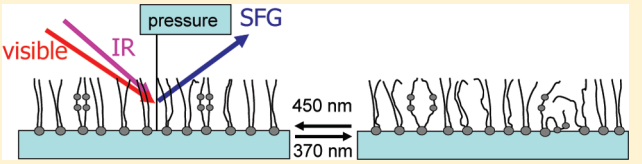

INTRODUCTION

Self-assembled monolayers of azobenzene-based surfactant molecules are uniquely photoswitchable interfaces, with potential applications as sensors in nanotechnology.[1−3] Switching the surfactants between the cis and trans states with light around 400 nm in wavelength can result in dramatic differences in surface pressure, surface potential, vesicle stability, and critical micelle concentration.[2,4−7] It has also been shown that embedding an azobenzene-based surfactant into an artificial membrane allows for external optical control over the activity of a mechanosensitive membrane-channel protein.[8] Understanding the molecular details behind the switching process is therefore also important for the development of artificial gating mechanisms, which might ultimately be used for applications in biology and medicine.[9] Despite its importance, a detailed molecular-level understanding of the switching process has been lacking.[5]

Herein, we investigate monolayers of the photoswitchable lipid DT Azo-5P (Figure 1), pure and mixed with the lipid 1,2-dipalmitoyl-*sn*-glycero-3-phosphocholine (DPPC). The photoactive lipid can be switched from its trans to cis state and back with 370 and 450 nm light, respectively, as shown in the UV/vis spectra in Figure 1. We use surface pressure measurements in combination with label-free, broadband vibrational sum-frequency generation (VSFG) spectroscopy.[10] These techniques allow us to study a monolayer of lipid molecules on the air−water interface. Information about the interaction of the lipids with water molecules can be obtained as well as the molecular structure of the lipids. In the nonlinear optical technique VSFG, an infrared (IR) beam and a visible (VIS) beam are combined at the interface, resulting in a signal with the sum frequency of the two incoming beams. If the infrared is in resonance with a molecular vibration, the signal is strongly enhanced. It has been shown that this technique via the molecular vibrations provides information about the molecular conformation and orientation of lipids.[11−18] Sum-frequency generation is forbidden in centrosymmetric media, because it is a second-order nonlinear optical process.[19] Therefore, this technique is sensitive to the outermost surface molecular layer of a centrosymmetric material, such as an aqueous surface. Inversely, the lack of a signal is an indication that the material or molecular groups at the interface are centrosymmetric. For azobenzene-functionalized self-assembled monolayers on gold, SFG has been very useful in determining the cross-section and the mechanism of the photoisomerisation. It is concluded that the photoisomerization is driven by a direct electronic excitation, analogous to azobenzene in the liquid phase.[3]

We will show that by switching the photolipid, the surface pressure and the molecular ordering of the lipids can be reversibly controlled. In a mixed monolayer containing both photolipids and the lipid DPPC, we can control the ordering of DPPC by optically switching the azobenzene-based lipid. This provides a new means of externally controlling lipid−lipid interactions.

Received: November 30, 2010
Revised: January 20, 2011
Published: February 18, 2011

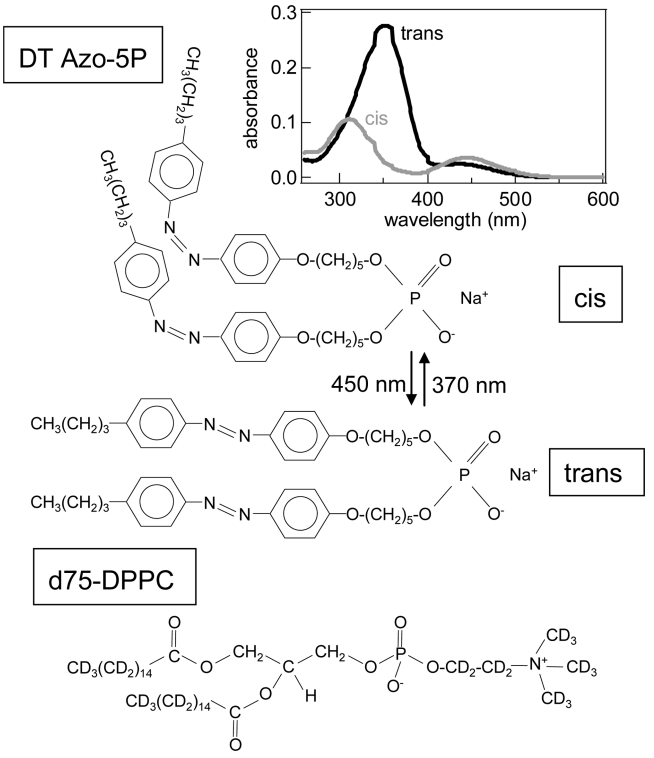

Figure 1. Molecular structure of the photoswitchable lipid DT Azo-5P in the cis and trans configuration and d75-DPPC. The inset in the top right corner shows the UV/vis spectra for the DT Azo-5P in $CHCl_3$ (~7 μM, 1 cm cuvette) after irradiation for roughly 10 s with 370 nm (cis state) and 450 nm (trans state).

EXPERIMENTAL SECTION

Sample. The synthesis of the azobenzene-containing dialkyl phosphates DT Azo-3P, DT Azo-5P, and DT Azo-9P has been described previously.[20] Monolayers of DT Azo-5P (or −3P and −9P) were spread from a 0.6 mM chloroform solution on an air-H_2O (Millipore, 18 MΩ/cm^{-1}) interface in a homemade trough of 7 by 7 cm^2 in the VSFG experiments and in a commercial metal Langmuir trough of 6 by 23 cm^2 (Kibron Inc., Finland) for the isotherm measurements. Normal DPPC and d75-DPPC (Figure 1) were obtained from Avanti Polar Lipids and both dissolved in chloroform to a concentration of roughly 0.7 mM. Mixtures of two lipids were made by mixing solutions of each compound before spreading on the surface. The area per molecule was controlled by the number of 0.5 μL droplets spread on the water surface. Diodes emitting at central wavelengths of 370 and 450 nm with a power of 8.3 and 21 mW, respectively, were used to switch between the two conformations of the photoswitchable lipid, as shown in Figure 1. We will refer to the system following 370 and 450 nm irradiation as the "cis" and "trans" states, respectively, although there will always be a mixture of conformers. The cis state can be obtained relatively pure as the absorption difference between trans and cis is very large around 370 nm. If one assumes that the cis state has zero absorbance at 390 nm (Figure 1), a small absorbance at this wavelength is caused by the trans state present in the cis state. As the absorbance at 390 nm is 5% from the fully thermally equilibrated trans spectrum, we conclude that at most 5% trans molecules are contributing to the overall absorption spectrum. If the cis state has a small absorption at 390 nm, the fraction of trans molecules present is even lower than this 5%. However, the absorption contrast between the cis and trans conformers at 450 nm is not so large, resulting in some cis molecules present in, what we will refer to here as, the trans state. The trans state will be "contaminated" with cis molecules. As the trans-state is thermally favorable, the irradiation-equilibrium will shift more to the trans state lowering the cis pollution. From a comparison of the UVvis absorption spectra of a fully thermally equilibrated trans state with the spectrum immediately after irradiation with 450 nm for half a minute the amount of cis pollution can be extracted from the observation that the latter spectrum can be constructed by 0.75 times the fully thermally equilibrated trans spectrum and 0.25 times the cis spectrum. From this we conclude that at most 25% cis "pollution" is present in the trans state. Both the UV and SFG spectra of the cis state are not changing in 30 min, if the sample is kept in darkness: apparently the thermal transition from cis to trans is slow. The quantum yield for both the trans−cis and cis−trans isomerization is wavelength-dependent and amount to typically tens of percent. (see, e.g., ref 21).

Setup. *Surface Pressure Measurements.* Surface pressures were measured with a commercially available tensiometer (Kibron, Finland) using a needle as probe. In the compression isotherm experiments the layer was compressed at a rate of ~7 Å^2/molecule/minute with two moving barriers. In the isotherm experiment, the cis state of the molecule was prepared by irradiating the sample with 370 nm light for roughly 60 s before spreading it on the surface.

Vibrational Sum-Frequency Generation Spectroscopy. The vibrational sum-frequency generation experiments were performed using visible pulses (12540 cm^{-1}, ~20 μJ, bandwidth of 17 cm^{-1}, full width at half-maximum, fwhm) overlapping with broadband infrared pulses (centered at 2160 or 2960 cm^{-1} to investigate C−D and C−H stretch modes, respectively, with a pulse energy of ~5 μJ, and a fwhm bandwidth of 150 cm^{-1}). These infrared pulses were generated by an OPG/OPA (TOPAS, Light Conversion) pumped by part of the output of a ~100 fs amplified Ti:sapphire laser system (Legend, Coherent, Inc.). The narrow band VIS pulse provides the spectral resolution of the experiments, while the broad band IR pulse allows the detection of a multitude of vibrational modes at once.[10,22] To correct for the frequency dependency of the IR power, the VSFG spectra were normalized by a reference spectrum taken from z-cut quartz. The incident angles of the VIS and IR beams were respectively 35° and 40° with respect to the surface normal. Both beams were focused down to approximately 100 μm beam waist. The fluence of the visible beam is low enough to avoid two-photon isomerization of the azobenzene moiety, which is checked by comparing spectra before and after some time of irradiation. The VSFG light was spectrally dispersed by a monochromator and detected by an Electron-Multiplied Charge Coupled Device (EMCCD, Andor Technologies). The VSFG spectra were recorded, unless stated otherwise, under s-polarized VSFG, s-polarized VIS, and p-polarized IR (SSP) conditions in 60 s for the pure DT Azo-5P experiment and in 180 s for the mixtures. In the experiments where we alternated between the cis and trans state, the diodes irradiated the system from above. The light from the diodes was unfocused and it irradiated almost the whole trough, so that distortion of the signal due to diffusion of lipids from outside the irradiation area into the laser focus is not a significant factor. Both the pressure meter and the laser focus were located well inside the area the diodes irradiate. We irradiated always for at least 100 s (corresponding to 1.5 ×

dx.doi.org/10.1021/jp1113619 |J. Phys. Chem. B 2011, 115, 2294–2302

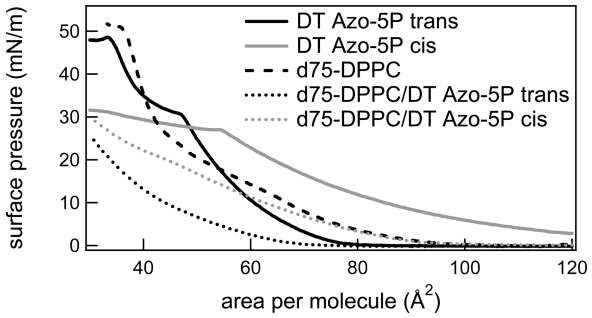

Figure 2. Surface pressure versus area isotherm for the photoswitchable lipid DT Azo-5P in both the trans and cis state (solid lines), for d75-DPPC (dash lines), and for a 1:5 molar ratio of photoswitchable lipid and d75-DPPC in the two states of the photoswitch (dotted lines).

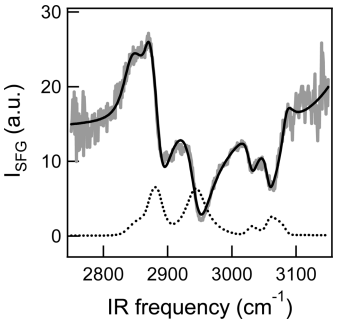

Figure 3. VSFG spectra in the CH region for DT Azo-5P in the trans state, at a density of 75 Å^2/molecule and a pressure of ~3 mN/m. The resonant signal is superimposed on a large nonresonant background, giving rise to dispersive lineshapes due to interference between resonant and nonresonant signals. The dotted black curve represents the DT Azo-5P signal for the case that the NR amplitude was set to zero.

10^{18} and 4.8×10^{18} photons for 370 and 450 nm, respectively) to obtain maximal conversion, which is apparent from a kinetic study: irradiating longer than 100 s does not change the pressure and the VSFG signal anymore.

RESULTS AND DISCUSSION

Surface Pressure. Before presenting VSFG spectra, we first report the pressure−area isotherm of the different monolayers. Figure 2 shows isotherms for DT Azo-5P in both states of the photoswitch. On the basis of the generalized isotherm given by Kaganer et al.,[23] containing gas (G), liquid expanded (LE), and condensed phases, we give a tentative assignment for the isotherms. Upon compression of DT Azo-5P in its thermally stable trans state, a transition occurs when the surface pressure becomes finite below roughly 80 Å^2 per molecule. This transition is assigned to a transition from the LE/G coexistence region to the LE phase. A second pressure discontinuity was observed at 50 Å^2 per molecule, indicating a transition from the LE into the LE/condensed coexistence before the condensed phase is formed. At a density around 30 Å^2 per molecule, the monolayer collapses.

The isotherm for the photolipid in the cis state (irradiated with 370 nm light before deposition on the water surface) looks very different. First of all, the pressure is finite already at much lower densities. This is in accordance with earlier observations for azobenzene-containing molecules[2,24] and most likely originates from the larger molecular footprint of *cis*-molecules.[8] A larger molecular footprint implies that interlipid interactions, and the onset of finite surface pressure, will occur at lower densities for the cis than for the trans isomers. Second, a transition occurs at 55 Å^2 per molecule, which might indicate the transition from a LE phase to a more condensed phase. At areas below 50 Å^2 per molecule, the pressure in the trans state is significantly higher than that in the cis state.

The isotherm for d75-DPPC shows the characteristic phases for lipid monolayers:[23] G/LE coexistence above 100 Å^2 per molecule, LE until roughly 60 Å^2, then a plateau (which is not very flat in this case, due to the relative high compression speed) of the coexistence of the LE and condensed phases, and finally the condensed phase below roughly 45 Å^2 per molecule.

The isotherm of the 5:1 DPPC/DT Azo-5P mixture lies consistently below the isotherms of the separated molecules. If the two different lipids are present on the surface in well-separated domains or if they are ideally mixed without interacting, one expects the isotherm of the mixture to be a simple sum of the isotherms of the pure lipids.[25,26] Clearly, this is not the case here, indicating that the two lipids are miscible and form nonideal mixed monolayers. Since at any pressure the area per molecule of the mixture is lower than the sum of the fractional areas of the two pure substituents, it can be concluded that the two types of lipids have an attractive interaction,[25] that can have different origins. First, the positive charge on the DT Azo-5P headgroup and the zwitterionic charge on the DPPC might result in a more attractive interaction between DPPC and DT Azo-5P than between lipids of the same sort. Second, in the mixture, the headgroup region might be dewatered resulting in closer packing, and third, the shape of both lipids is different: cone and cylindrical for DT Azo-5P and DPPC, respectively. This might also result in a denser packing geometry in case of the mixture.

Vibrational Sum-Frequency Generation Spectroscopy (VSFG) of DT Azo-5P Monolayers. Figure 3a depicts in gray VSFG spectra for a monolayer in the condensed phase of the photolipid DT Azo-5P in the trans state at a surface pressure of 3 mN/m and a molecular area of 75 Å^2. The spectrum shows resonances for the CH_2 (~2840 cm^{-1}) and CH_3 symmetric stretch mode (~2860 cm^{-1}), the CH_2 and CH_3 asymmetric stretch modes at ~2890 and 2940 cm^{-1}, and above 3000 cm^{-1} aromatic CH-signals, originating from the azobenzene moiety.[2,11−13] Above 3100 cm^{-1}, the spectrum is dominated by the OH vibrations from the water subphase. The spectrum has an unusual high (nonzero) baseline at low frequency, which indicates a high nonresonant signal. To check this possibility the spectrum is fitted using the following expressions:[11,12]

$$\begin{aligned} I_{SFG}(\omega_{IR}) &\propto |\chi^{(2)}(\omega_{IR})|^2 I_{VIS} I_{IR} \\ &\propto |\chi^{(2)}_{NR} + \chi^{(2)}_{R}(\omega_{IR})|^2 I_{VIS} I_{IR} \\ &\propto (\chi^{*(2)}_{NR}\chi^{(2)}_{NR} + \chi^{*(2)}_{NR}\chi^{(2)}_{R}(\omega_{IR}) + \chi^{(2)}_{NR}\chi^{*(2)}_{R}(\omega_{IR}) \\ &\quad + \chi^{*(2)}_{R}(\omega_{IR})\chi^{(2)}_{R}(\omega_{IR}))I_{VIS} I_{IR} \end{aligned} \quad (1)$$

with

$$\chi^{(2)}_{NR} = A_0 e^{i\varphi}$$

$$\chi^{(2)}_{R}(\omega_{IR}) = \sum_n \frac{A_n}{\omega_{IR} - \omega_n + i\Gamma_n}$$

The susceptibility contains a nonresonant term, with amplitude A_0 and phase relative to the resonant term φ, and a resonant one. The latter describes the n vibrational resonances by their resonance frequencies ω_n, line widths $2\Gamma_n$, and amplitudes A_n.

dx.doi.org/10.1021/jp1113619 |*J. Phys. Chem. B* 2011, 115, 2294–2302

The relative sign of the amplitudes of the resonant terms is taken from literature.[12,27,28] The fit result is depicted in Figure 3 in black. Indeed, the fit reveals a 3 times larger nonresonant amplitude for the DT Azo-5P than that commonly observed for lipid monolayers, such as DPPC (see below). The effect of the large nonresonant contribution to the signal is illustrated by the black dotted curve in Figure 3a, which represents a calculated spectrum for which the resonant response of the DT Azo-5P was used (obtained from the fit result), but with the nonresonant amplitude set to zero (and the water amplitude was set to zero from which the tail acts as a NR signal as well in the CH region). When the NR amplitude is set to zero, we observe not only that the background is lowered, but also a reduction of the apparent resonant signal size by a factor of 2 to 5, depending on the IR frequency. Similar signal enhancements due to electronic transitions have been observed by measuring VSFG spectra from Rhodamine 6G.[29,30] However, in that case the authors used visible light in resonance with an electronic excitation so that they performed a doubly resonant experiment. For the DT Azo-5P there is no electronic transition at 800 nm, so there is no double resonance effect; the enhancement is purely nonresonant. Hence, for the present system, the nonresonant signal heterodynes the resonant signal due to cross-terms from the $\chi^{(2)}_{NR}$ and $\chi^{(2)}_{R}$ (see the second and third term in the last line of eq 1), and enhances the signal rather than affecting $\chi^{(2)}_{R}$ directly, as concluded for Rhodamine 6G.[29,30] The heterodyning effect is therefore not only intramolecular, but also intermolecular, and can be straightforwardly used to boost low signals in highly diluted samples, by, for example, simply adding benzene-containing moieties to a monolayer. This implies that the signal size in the VSFG spectrum is in this case not simply quadratically dependent on the number of molecules as in most cases where the nonresonant contribution is very small. In the Appendix, we demonstrate that relatively low levels of DPPC can be measured in the presence of the photolipid, owing to the heterodyning. This nonresonant heterodyning may provide a useful means of detecting the vibrational response of low concentrations of molecules in molecular monolayers.

Vibrational Sum-Frequency Generation Spectroscopy (VSFG) of DT Azo-5P in Cis and Trans States. To obtain information about the molecular structure of the lipids in the different states, VSFG spectra were measured during an irradiation cycle. The lipid molecular vibrations provide direct information about the molecular conformation, orientation, and order.[11−18] A typical surface pressure measurement during an irradiation cycle is depicted in Figure 4a for a pure DT Azo-5P monolayer at a surface density of 75 Å^2 per molecule. The sample, spread as a mixture of cis and trans isomers, was sequentially irradiated with 370 and 450 nm for ∼100 s each. After irradiating with 370 nm the pressure rose to 16 mN/m, while 450 nm irradiation caused a pressure drop down to 3 mN/m, in agreement with a vertical transition between the two isotherms in Figure 2. Figure 4b shows the VSFG spectra in the CH region for the cis and trans states, respectively, which intrinsically exhibit high and low surface pressure, respectively. On top of a nonresonant background (the horizontal black lines mark zero), the spectra of both the cis and trans configurations reveal aliphatic CH_2 and CH_3 modes of the alkyl chains below 3000 cm^{-1} and aromatic CH stretch modes above 3000 cm^{-1} [2,11−13] as assigned above. In addition, a signal from the OH vibration of the underlying water is apparent above 3100 cm^{-1}. A larger part of the water spectrum is depicted in Figure 4c, showing that the water signal is roughly 1.4 times larger in the trans state than in the cis state yet is similar in its spectral shape.

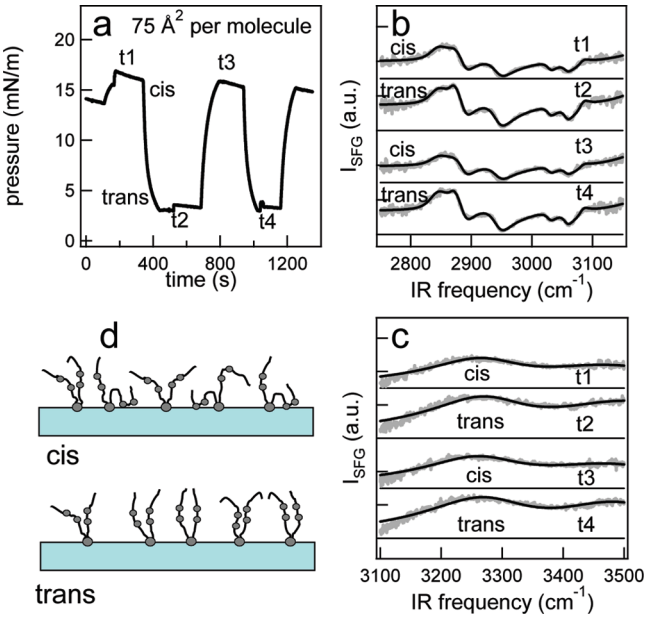

Figure 4. (a) Surface pressure as a function of time for the photoswitchable lipid at the lipid/H_2O interface at an area of 75 Å^2 per molecule. Irradiation with 370 and 450 nm light for ∼100 s created the cis (high pressure) and trans (low pressure) state, respectively. The small sharp fluctuations in the pressure are due to changes in the height of the sample to correct for evaporation of the water. (b and c) Corresponding VSFG spectra in the CH and OH region (gray) together with fits to a Lorenztian line shape model (see text). The spectra have been offset for clarity. t1 to t4 correspond to the time in panel a at which the spectra were taken. (d) Schematic representation of the orientation of the lipid tails. The azobenzene moieties of the photoswitchable lipid are represented as gray circles.

The molecular order in the lipid tails can be obtained from the VSFG response in the C−H stretch region. For an ordered monolayer of phospholipids, the VSFG intensity of the methylene CH_2 is low and the methyl CH_3 stretch intensity is high, due to, respectively, the inversion symmetry of an all-trans alkyl chain that leads to cancellation of the methylene CH_2 dipoles and collective orientation of the methyl groups, leading to the efficient coherent addition of the methyl CH_3 dipoles. On the other hand when gauche defects are formed, the inversion symmetry within the alkyl chain is broken and the relative intensity of the methylene symmetric stretch mode increases; simultaneously, the disorder reduces the methyl intensity. As such, the order of lipids at the air−water interface can be quantified through the intensity or amplitude ratio of the methyl and the methylene groups in the lipid alkyl chains.[31] Switching between the trans and cis state of the photolipid, the CH_2 symmetric stretch (2848 cm^{-1}) and the CH_3 symmetric stretch (2871 cm^{-1}) indeed show differences, as evident from Figure 4b. In particular, a higher CH_3/CH_2 ratio is observed in the trans case, indicating a higher order in the alkyl chain, despite the lower pressure. This higher molecular order observed in the trans-state is in agreement with MD simulations that show that the tails are more elongated in the trans-state.[8,32]

To obtain more quantitative information about peak amplitudes and about the molecular ordering of the lipid tails, the

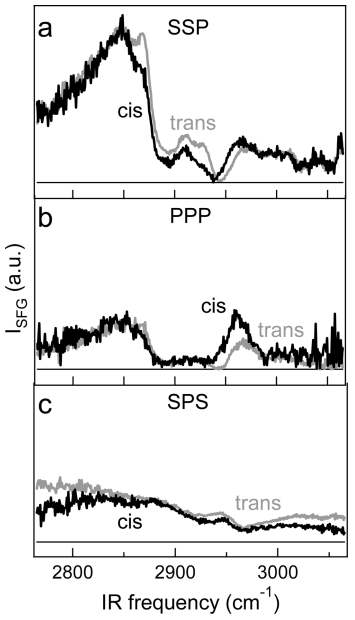

Figure 5. (a) Normalized VSFG spectra with SSP polarization for a pure monolayer of DT Azo-5P at an area of 65 Å^2 per molecule in the trans and cis state for P is 6 and 20 mN/m, respectively. (b) Like part a, but for PPP polarization. (c) SFG spectra in the SPS polarization for the trans and cis state (~78 Å^2 per molecule) at a pressure of 2 and 15 mN/m. The three panels have the same vertical scale.

spectra are fitted using the model discussed above. The fit results are depicted as black lines in Figure 4b. From the amplitudes of the different Lorentzian peaks in the fit we clearly find that for the symmetric stretch mode, the CH_3/CH_2 amplitude ratio is 6 ± 3 times higher in the trans state than in the cis state. A similar fit (Figure 4c, black lines) to the water signal shows that the increase in nonresonant signal is not the cause for the higher water signal in the trans case, because the resonant contribution is much larger than the nonresonant. The intensity of the resonant water response is 1.4 times higher for the trans state than for the cis.

To unravel whether the molecular orientation changes upon switching, experiments were performed at different polarizations. The results are depicted in Figure 5. The difference between trans and cis is more pronounced than that for the data from Figure 4, because the lipid density is higher. The PPP data (Figure 5b) show the same behavior as those for the SSP: upon going from trans to cis the CH_3 symmetric and asymmetric stretch is reduced. The first is visible as a decrease in the spectrum at 2860 cm^{-1}, while the second one results in the decreased dip at 2940 cm^{-1} (due to the negative amplitude the peak is appearing as a dip). The SPS spectrum, taken at slightly lower density, shows minor differences. Clearly, the three different polarizations show the same trend, from which we conclude that there is no major collective reorientation of molecules within the monolayer occurring in the system.

We would like to infer a picture of the molecular conformation from our data. Such a picture would have to consistently explain the following observations for the trans and cis states: (i) increased molecular order in the trans state, despite the (ii) lower pressure for the trans state and (iii) a larger water signal for the trans state. As a larger water signal implies that more water molecules are aligned, we can conclude that in the trans-case the water underneath the negatively charged lipid is more aligned than in the cis case. In general, the charge of the headgroup determines the amount of water aligned due to the electrostatic potential: all other things being equal, charged lipids align more water than zwitterionic lipids. (see, e.g., ref 28) The main difference between cis and trans is the dipole moment around the azobenzene moiety, which is 4.5 and 1.3 D for cis and trans azobenzene, respectively.[33] The higher dipole moment in the cis state makes interaction with the water more favorable.[5] Apparently, part of the azobenzene moieties interacts with the water in the cis case in such a way that it lowers the water signal, presumably by decreasing the surface potential at the interface. These observations can be accounted for when the large dipole in the cis-azobenzene group comes sufficiently close to the surface to screen part of the negative charge in the phosphate headgroup. The dipole moment of the azobenzene moiety is oriented perpendicular to the N═N bond. For the dipole to orient itself perpendicular to the surface plane, the lipid tail must form a loop, which has indeed been proposed previously for an azobenzene-based neutral surfactant[5] and for an azobenzene-containing polymer.[2] This situation is schematically depicted in the top panel of Figure 4d. The loop formation also explains the higher pressure in the cis state compared to the trans state, because of the large increase in the footprint of the molecules. Most likely, in the trans state $\pi-\pi$ bonding is more favorable than interaction with the water. This scenario of loop formation in the cis case and elongated chains in the trans case also accounts for the observations of increased order in the lipid tails in the trans case. In summary, the lower order, lower water signal and higher pressure in the cis state are all in agreement with a molecular picture where at least part of the lipid tails form a loop so that the *cis*-azobenzene group with its large dipole moment is in (near-) contact with the water. In the trans state the tails are more elongated and not in contact with the water. A sketch of a possible molecular picture is given in Figure 4d.

For DT Azo-3P the VSFG spectra are similar to those for DT Azo-5P. These molecules differ in the position of the azobenzene moiety in the chain: DT Azo-5P and DT Azo-3P have the azobenzene moiety 5 and 3 CH_2 groups away from the headgroup, respectively. We observe the same spectral features in the spectra from both molecules and the order is higher for both lipids in the trans state. For a lipid with the azobenzene group at the end of the tail (DT Azo-9P) the spectra in the cis and trans states are indiscernible; apparently the lipid ordering is not affected if the molecular switch is located completely at the end of the tails. The heterodyning effects described above are very similar for DT Azo-3P, DT Azo-5P, and DT Azo-9P.

Mixtures of DT Azo-5P and DPPC. To investigate the effect of switching DT Azo-5P on the conformational behavior of conventional lipids, we prepared monolayers consisting of a mixture of DPPC and DT Azo-5P. To be able to readily distinguish the different lipids, we used in these experiments, d75-DPPC and nondeuterated DT Azo-5P. In this way, we can discriminate the molecular vibrations of the two different lipids to a large extent. Unfortunately, d75-DPPC still has 5 H atoms present in the molecule (Figure 1), which gives a VSFG signal as can be observed by looking at the bottom curve in Figure 6c and 7c which shows the spectrum for pure d75-DPPC (fully deuterated DPPC is not commercially available). The peak at around 2960 cm^{-1} in Figure 6c originates from the vibrations of these CH groups located between the headgroup and the tail of d75-DPPC. This peak is absent in the pure photolipid monolayer

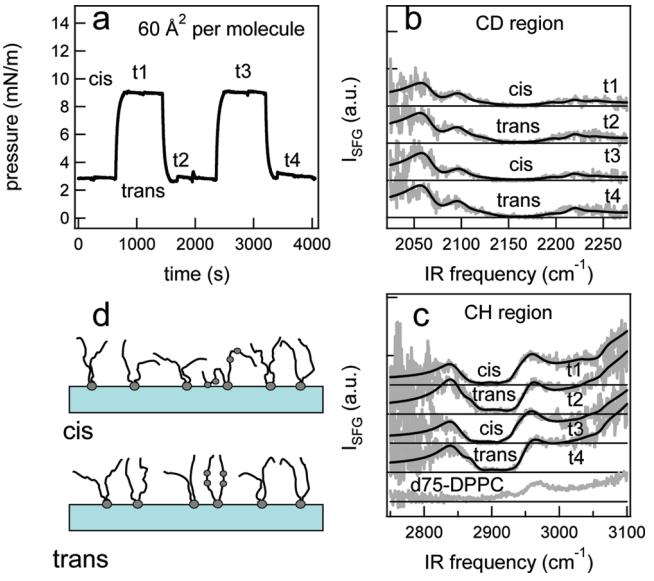

Figure 6. Results for the 1:5 mixture of DT Azo-5P/d75-DPPC at the lipid/H_2O interface at an area of 60 Å^2 per molecule. (a) Surface pressure vs time. Irradiation with 370 and 450 nm light for ∼100 s created the cis (high pressure) and trans (low pressure) state, respectively. The small sharp fluctuations in the pressure are due to changes in the height of the sample to correct for evaporation of the water. (b) Corresponding VSFG spectra (gray) together with fits in the CD region. The spectra have been offset for clarity. (c) VSFG spectra (gray) together with fits to guide the eye in the CH region. The bottom curve shows the spectrum for pure d75-DPPC at $P \sim 40$ mN/m. (d) Schematic representation of the orientation of the lipid tails. The azobenzene moieties of the photoswitchable lipid are represented as gray circles.

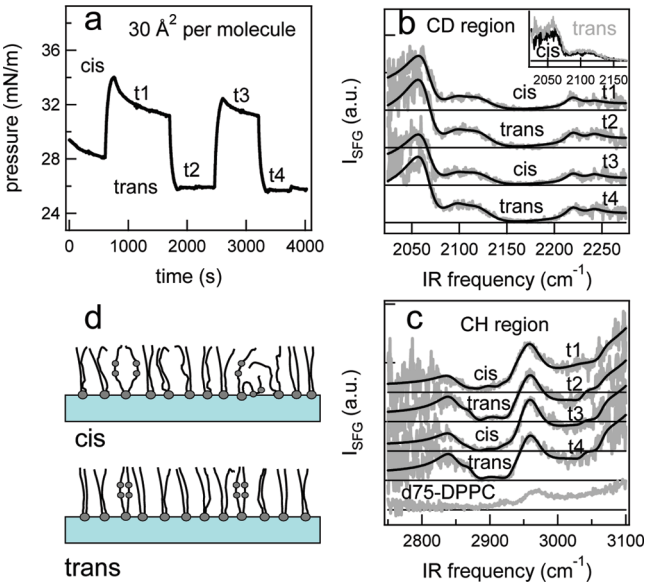

Figure 7. Results for the 1:5 mixture of DT Azo-5P/d75-DPPC at the lipid/H_2O interface at an area of 30 Å^2 per molecule. (a) Surface pressure vs time. Irradiation with 370 and 450 nm light for ∼100 s created the cis (high pressure) and trans (low pressure) state, respectively. The small sharp fluctuations in the pressure are due to changes in the height of the sample to correct for evaporation of the water. The decrease in the surface pressure in the cis state might be due to relaxation of the monolayer or the formation of micelles or vesicles reducing the amount of lipids at the surface. (b) Corresponding VSFG spectra (gray) together with fits in the CD region. The spectra have been offset for clarity. The inset shows the trans and cis spectra on top of each other to emphasize the difference. (c) VSFG spectra (gray) together with fits to guide the eye in the CH region. The bottom curve shows the spectrum for pure d75-DPPC at $P \sim 40$ mN/m. (d) Schematic representation of the orientation of the lipid tails. The azobenzene moieties of the photoswitchable lipid are represented as gray circles.

(Figure 4b). Figure 6a shows an irradiation cycle for a 5:1 mixture of d75-DPPC/DT Azo-5P at 60 Å^2 per molecule. The surface pressure alternates reproducibly between 3 and 9 mN/m. Corresponding VSFG spectra in both the CD and CH spectral range are depicted in Figure 6b and c, respectively. The spectra in the CD range match quite well the spectra previously reported for pure d62-DPPC[34] indicating that the CH_3 groups of the headgroup (the choline group) have a negligible contribution to the spectrum: only vibrational modes of the tails are visible. The different peaks can be assigned as follows: CD_3 symmetric stretch (2066 cm^{-1}), CD_2 symmetric stretch (2100 cm^{-1}), CD_3 Fermi resonance (2124 cm^{-1}), CD_2 asymmetric stretch (2195 cm^{-1}), and CD_3 asymmetric stretch (2218 cm^{-1}). The presence of the photoswitchable lipid manifests itself in the higher nonresonant background compared to pure DPPC as described above. At this low density of photolipids the differences between the SFG spectra observed for the trans and cis states of the photoswitchable lipid are clearly less pronounced than for the pure monolayer, both in the CD (DPPC) and CH (DPPC and photolipid) regions. The spectra in the CH region (Figure 6c) are dominated by the water band above 3000 cm^{-1}, a peak from the DPPC at 2960 cm^{-1}, and the CH_2 and CH_3 symmetric stretch vibrations of the photoswitchable lipid around 2850 cm^{-1}. Since only roughly 17% of the molecules present at the surface are the photoswitchable lipid and, to a first order approximation, the VSFG signal depends quadratically on the number of molecules, it is obvious that the vibrations of these molecules are not pronounced in the spectrum. At higher overall density (but constant DPPC:DT Azo-5P ratio) the differences between the cis and trans states are larger, as can be seen in Figure 7, parts b and c, where the density is 30 Å^2 per molecule and the pressure alternates between 26 and 32 mN/m (Figure 7a). The amplitudes of the different peaks are higher if the photoswitchable lipid is present in the trans-state, which is partly due to a higher NR background in the trans state.

To get a more quantitative view of the molecular ordering, the amplitudes of the CD_3 and CD_2 symmetric stretch modes of DPPC for four different densities are given in Figure 8, parts a and b, from fits such as shown in Figure 6b and 7b (black lines). As expected, in both cis and trans states the CD_3 amplitude increases and the CD_2 amplitude decreases with increasing density (lower area per molecule), shown in different colors in the plot. This is due to the straightening of the alkyl chains by reducing the number of gauche defects with increasing density. With increasing density, the order increases, as does the surface pressure. Remarkably, when the pressure is increased by going from trans to cis (rather than by increasing the surface coverage), the anticorrelation between the CD_3 and CD_2 remains, but now an increase in pressure makes that the CD_3 amplitude goes *down*, and the CD_2 amplitude *goes up* (we note that the latter conclusion is somewhat tentative, given the error bars on the experimental data points). To emphasize this counterintuitive behavior of the DPPC/DT Azo-5P mixture, the right panel of Figure 8 shows the fit results for pure normal DPPC for the same

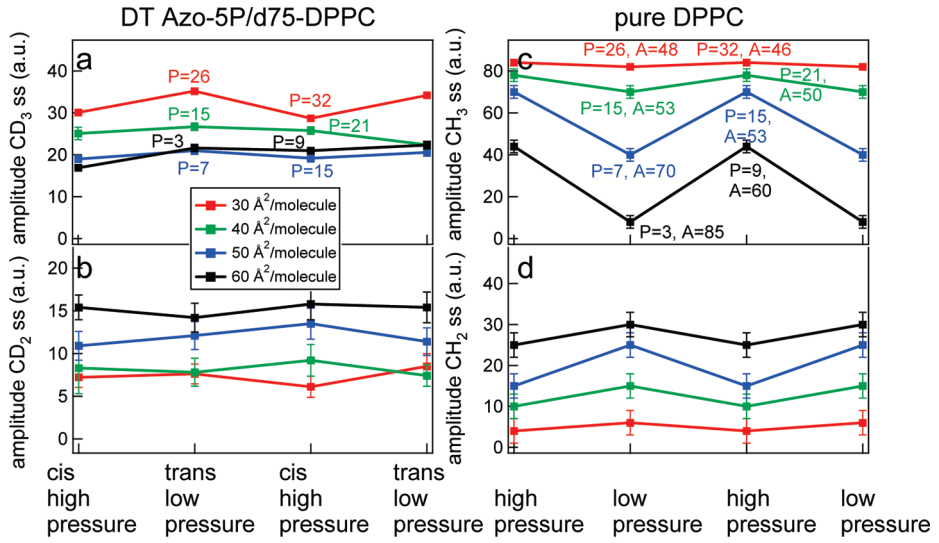

Figure 8. Fit results for d75-DPPC in the experiments with the 5:1 ratio of d75-DPPC and DT Azo-5P (left) and for pure normal DPPC (right). (a) Amplitude of the CD_3 symmetric stretch vibrational mode as a function of the state of the photoswitchable lipid for different densities; (b) amplitude of the CD_2 symmetric stretch vibrational mode as a function of the state of the photoswitchable lipid for different densities; the right panel shows similar results for pure DPPC for comparable pressure as those for the left panel, with (c) amplitude of the CH_3 symmetric stretch vibrational mode and (d) amplitude of the CH_2 symmetric stretch mode. The width and frequency of the resonances are fixed in the fit.

corresponding pressures. Every data point in the right panel mimics the pressure of the points in the left panel; we compare pressures, rather than densities. Clearly, the effect of changing the pressure is much larger for pure DPPC than for the mixture. Already at very low pressure ($P = 3$) there is a clear signal for the CD_3 symmetric stretch mode in the mixture, but almost no signal for pure DPPC; the presence of the photoswitchable lipid induces higher order of the CD_3 groups already at very low pressure. For high pressure the CH_2 modes almost completely disappear for pure DPPC, while for the mixture there remains a clear CD_2 signal; the tails are less ordered if DT Azo-5P is present. This is not surprising, since the DT Azo-5P lipids will act as packing defects in the fully compressed DPPC monolayer. Moreover, at low density (pressure up to ~15 mN/m) the effects of changing the pressure are more dramatic for pure DPPC than for the mixture. Apparently, the photoswitchable lipid has a larger effect on the pressure than on the molecular ordering of the lipids.

An interesting observation is thus that the molecular disorder in the lipid monolayer—for the photolipids as well as for DPPC—increases with increasing pressure, when the pressure is increased by photoswitching. This is true for both the photolipid itself, but also for the mixture. This seems counterintuitive since one might expect that the increased lipid−lipid interaction at higher pressures would lead to more order in the alkyl chains. However, this phenomenon can readily be explained by noting the following: The surface pressure equals the decrease in surface free energy per unit area. The surface free energy is primarily determined by electrostatic and dipolar interactions of the lipids with the water interface and of the lipid headgroups with each other; the van der Waals interactions between the lipid alkyl chains are relatively weak. Hence, when the pressure is increased by compressing the monolayer, this is primarily a consequence of the increased electrostatic interactions at the interface, whereas the increase in van der Waals interactions between the alkyl chains, which serve to order those alkyl chains, are expected to remain relatively weak. However, the density does not increase when decreasing the surface free energy (increasing the surface pressure) by switching the photolipids from trans to cis. Rather, we attribute the lowering of the surface free energy (increases the pressure) in the cis-state by an increase in the electrostatic interactions at the water interface owing to its larger dipole. Therefore, our results indicate that the azobenzene dipoles approach the surface, resulting in an appreciable larger footprint for the cis- than the trans-state, possibly due to the formation of a loop in some of the tails. This means that effectively the headgroup region becomes more crowded, but the apolar region containing the alkyl chains becomes less dense, allowing for a larger conformational freedom of the alkyl chains, and less alkyl chain order. Hence, despite the pressure increase, the alkyl chain order is observed to decrease.

A schematic presentation of how the lipid trans−cis switching can simultaneously give rise to higher pressure and lower order is shown in Figures 6d and 7d.

CONCLUSION

We report here VSFG measurements to study the molecular structures in monolayers of the pure photoswitchable lipid DT Azo-5P and of mixtures of this photoswitchable lipid with the conventional lipid DPPC. Monolayers with DT Azo-5P in the cis state above 50 $Å^2$/molecule exhibit a higher pressure than monolayers with the trans state of the lipid, but exhibit less order in the alkyl chain. The cis state also exhibits a lower signal and has a larger footprint resulting in a larger pressure due to stronger electrostatic interactions at the interface owing to the interaction of the azobenzene dipoles with water, presumably resulting in loop formation of the lipid tail. The weaker VSFG signal of the water underneath the lipids in the cis state indicates that in this case the azobenzene moiety is in contact with the water partly diminishing the effect of the negative charge of the lipid headgroup. To be in contact with water the tails have to form a loop, resulting in the higher disorder.

For the mixture of the lipids, the effect of the state of the photoswitch is clearly present in the change of surface pressure,

dx.doi.org/10.1021/jp1113619 |J. Phys. Chem. B 2011, 115, 2294–2302

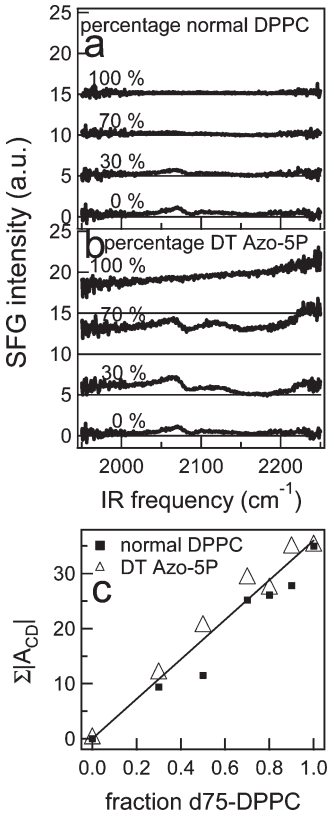

Figure 9. (a) VSFG spectra in the CD region for varying mixtures of normal DPPC and d75-DPPC. The percentage of normal DPPC in the mixture is given in the graph. The spectra are offset for clarity and the thin lines represent the zero. (b) Like part a, but for a mixture of DT Azo-5P with d75-DPPC. (c) The sum of the amplitudes of the CD vibrations obtained by fitting the VSFG spectra as described in the text as a function of the fraction d75-DPPC in a binary mixture with normal DPPC or DT Azo-5P. In this experiment the IR fluence was high in order to get good quality data for the mixtures, resulting in small disorder in the lipid tails observed via relatively high CH_2 and CD_2 amplitudes in the VSFG spectra.

but the differences on the molecular level between the cis and trans state of DT Azo-5P are less pronounced. However, at high density and thus high pressure, the amplitudes of the CD_3 and CD_2 stretch modes are behaving counterintuitively. In the lower pressure state, the trans state, the amplitude of the CD_3 mode is larger, and that of the CD_2 smaller, than in the higher pressure state. For a pure layer of DPPC a higher pressure always results in a higher signal for the CH_3 symmetric stretch mode and a lower signal for the CH_2 mode. Apparently, the presence of the photoswitch influences the structure of the lipid tails of DPPC in a different way as expected solely from just the change in pressure.

APPENDIX

To prove that the heterodyning effect is the cause of the signal enhancement, we have measured VSFG spectra for mixtures of DPPC and DT Azo-5P. To be molecule-specific we used in this experiment d75-DPPC and examined the CD vibrational region. As reference samples we used mixtures of normal DPPC (undeuterated) and d75-DPPC. In other words, we compare different mixtures of d75-DPPC and DT Azo-5P with mixtures of d75-DPPC and DPPC (undeuterated). The molar d75-DPPC/DT Azo-5P ratio is equal to the molar d75-DPPC/DPPC (undeuterated) ratio. We prepared the monolayer always in the same way, such that the area per molecule is ~35 Å^2 (condensed phase). The resulting VSFG spectra for d75-DPPC are shown in Figure 9, parts a and b, for different fractions of DPPC or DT Azo-5P present in the mixture. As expected for the d75-DPPC/DPPC (undeuterated) mixture (Figure 9a) the VSFG signal decreases roughly quadratically with increasing fraction of normal DPPC present in the layer. In this case the nonresonant term is small and the signal is therefore dominated by the last term in the last line of equation one ($I_{SFG} \propto \chi^{*(2)}_{R} \chi^{(2)}_{R} I_{VIS} I_{IR}$). For mixtures with DT Azo-5P, the effect is quite different. The background increases as the amount of DT Azo-5P increases and the signal size on top of the background is about constant although the amount of d75-DPPC decreases from bottom to top. By fitting the data with the above-mentioned model, we can extract the nonresonant and resonant contributions to the signal. The resonant contribution, given as the sum of the CD amplitudes, is depicted in Figure 9c as a function of the fraction d75-DPPC present in the mixture. Clearly, for both samples the amplitude increases linearly with the fraction of d75-DPPC present and both curves lie on top of each other. So, the presence of molecules with a strong NR signal influences only the nonresonant part, but, interestingly, it amplifies the signal from neighboring molecules.

AUTHOR INFORMATION

Corresponding Author
*E-mail: bonn@amolf.nl.

ACKNOWLEDGMENT

This work is part of the research program of the "Stichting voor Fundamenteel Onderzoek der Materie (FOM)", which is financially supported by the "Nederlandse Organisatie voor Wetenschappelijk Onderzoek (NWO)".

REFERENCES

(1) Kumar, A. S.; Ye, T.; Takami, T.; Yu, B.-C.; Flatt, A. K.; Tour, J. M.; Weiss, P. S. *Nano Lett.* **2008**, *8*, 1644.
(2) Ohe, C.; Kamijo, H.; Arai, M.; Adachi, M.; Miyazawa, H.; Itoh, K.; Seki, T. *J. Phys. Chem. C* **2008**, *112*, 172.
(3) Wagner, S.; Leyssner, F.; Kördel, C.; Zarwell, S.; Schmidt, R.; Weinelt, M.; Rück-Braun, K.; Wolf, M.; Tegeder, P. *Phys. Chem. Chem. Phys.* **2009**, *11*, 6242.
(4) Shin, J.; Abbott, N. L. *Langmuir* **1999**, *15*, 4404.
(5) Shang, T.; Smith, K. A.; Hatton, T. A. *Langmuir* **2003**, *19*, 10764.
(6) Tong, X.; Wang, G.; Soldera, A.; Zhao, Y. *J. Phys. Chem. B* **2005**, *109*, 20281.
(7) Eastoe, J.; Vesperinas, A. *Soft Matter* **2005**, *1*, 338.
(8) Folgering, J. H. A.; Kuiper, J. M.; Vries, A. H. d.; Engberts, J. B. F. N.; Poolman, B. *Langmuir* **2004**, *20*, 6985.
(9) Banghart, M. R.; Volgraf, M.; Trauner, D. *Biochemistry* **2006**, *45*, 15129.
(10) Arnolds, H.; Bonn, M. *Surf. Sci. Rep.* **2010**, *65*, 45.
(11) Roke, S.; Schins, J.; Müller, M.; Bonn, M. *Phys. Rev. Lett.* **2003**, *90*, 128101.
(12) Ji, N.; Ostroverkhov, V.; Chen, C.-Y.; Shen, Y.-R. *J. Am. Chem. Soc.* **2007**, *129*, 10056.
(13) Sovago, M.; Wurpel, G. W. H.; Smits, M.; Müller, M.; Bonn, M. *J. Am. Chem. Soc.* **2007**, *129*, 11079.
(14) Watry, M. R.; Tarbuck, T. L.; Richmond, G. L. *J. Phys. Chem. B* **2003**, *107*, 512.

(15) Kim, G.; Gurau, M. C.; Lim, S. M.; Cremer, P. S. *J. Phys. Chem. B* **2003**, *107*, 1403.
(16) Liu, J.; Conboy, J. C. *J. Am. Chem. Soc.* **2004**, *126*, 8894.
(17) Doyle, A. W.; Fick, J.; Himmelhaus, M.; Eck, W.; Graziani, I.; Prudovsky, I.; Grunze, M.; Maciag, T.; Neivandt, D. J. *Langmuir* **2004**, *20*, 8961.
(18) Tyrode, E.; Niga, P.; Johnson, M.; Rutland, M. W. *Langmuir* **2010**, *26*, 14024.
(19) Shen, Y.-R. *Nature* **1989**, *337*, 519.
(20) Kuiper, J. M.; Hulst, R.; Engberts, J. B. F. N. *Synthesis* **2003**, 695.
(21) Zimmerman, G.; Chow, L.; Paik, U. *J. Am. Chem. Soc.* **1958**, *80*, 3528.
(22) Richter, L. J.; Petralli-Mallow, T. P.; Stephenson, J. C. *Opt. Lett.* **1998**, *23*, 1594.
(23) Kaganer, V. M.; Möhwald, H.; Dutta, P. *Rev. Mod. Phys.* **1999**, *71*, 779.
(24) Seki, T.; Sekizawa, H.; Morino, S.; Ichimura, K. *J. Phys. Chem. B* **1998**, *102*, 5313.
(25) Dynarowicz-Latka, P.; Kita, K. *Adv. Coll. Interf. Sci.* **1999**, *79*, 1.
(26) Roche, Y.; Peretti, R.; Bernard, S. *Biochim. Biophys. Acta* **2006**, *1758*, 468.
(27) Nihonyanagi, S.; Yamaguchi, S.; Tahara, T. *J. Chem. Phys.* **2009**, *130*, 204704.
(28) Chen, X.; Hua, W.; Huang, Z.; Allen, H. C. *J. Am. Chem. Soc.* **2010**, *132*, 11336.
(29) Raschke, M. B.; Hayashi, M.; Lin, S. H.; Shen, Y. R. *Chem. Phys. Lett.* **2002**, *359*, 367.
(30) Wu, D.; Deng, G. H.; Guo, Y.; Wang, H. F. *J. Phys. Chem. A* **2009**, *113*, 6058.
(31) Messmer, M. C.; Conboy, J. C.; Richmond, G. L. *J. Am. Chem. Soc.* **1995**, *117*, 8039.
(32) Kuiper, J. M.; Stuart, M. C. A.; Engberts, J. B. F. N. *Langmuir* **2008**, *24*, 426.
(33) Han, M. R.; Hirayama, Y.; Hara, M. *Chem. Mater.* **2006**, *18*, 2784.
(34) Ma, G.; Allen, H. C. *Langmuir* **2006**, *22*, 5341.